Properties of Mixed-Ligand Cyclometalated Platinum(II) Complexes Derived from 2-Phenylpyridine and 2-(2'-Thienyl)pyridine. Voltammetric, Absorption and Emission Studies

Per-Inge Kvam,[a, †] Michael V. Puzyk,[b] Vladimir S. Cotlyr,[b] Konstantin P. Balashev[b] and Jon Songstad[a]

[a]Department of Chemistry, University of Bergen, N-5007 Bergen, Norway and [b]Department of Chemistry, Russia State Pedagogical University, 191186 St. Petersburg, Russia

Kvam, P.-I., Puzyk, M. V., Cotlyr, V. S., Balashev, K. P. and Songstad, J., 1995. Properties of Mixed-Ligand Cyclometalated Platinum(II) Complexes Derived from 2-Phenylpyridine and 2-(2'-Thienyl)pyridine. Voltammetric, Absorption and Emission Studies – Acta Chem. Scand. 49: 645–652 © Acta Chemica Scandinavica 1995.

The spectroscopic and electrochemical properties of some cyclometalated Pt(II) complexes derived from 2-phenylpyridine, [Pt(ppy)AB], and 2-(2'-thienyl)pyridine, [Pt(tpy)AB], have been compared. A and B represent various monodentate and bidentate ligands.

When exchanging ppy with tpy the metal-to-ligand charge transfer, MLCT, as viewed by the structured absorption and emission bands, is shifted by ca. 3000 cm^{-1} to lower energy. The redox potentials for the two series of complexes, however, are most similar and depend only on the additional ligands A and B. The radiative lifetimes of the lowest excited state of the tpy complexes are significantly longer than for the ppy complexes. The various data indicate that the lowest excited state of the tpy complexes has a larger contribution from the π-character of the cyclometalated ligand. Since tpy complexes, contrary to most ppy complexes, are luminescent even at room temperature, it is concluded that this class of complexes are better candidates for promoting luminescent species.

The redox potentials of the complexes are linearly related to Lever's electrochemical parameters, E_L, with a slope of ca. 0.55 for reduction and ca. 0.65 for oxidation. The linear relationship breaks down for oxidation potentials when A and B represent sterically hindered phosphines, presumably due to oxidation of the heteroatoms.

The design and study of luminescent transition-metal complexes is currently of great interest. The mere phenomenon of luminescence indicates that a compound, in solution or in the solid state, is excited by light at some wavelength. The absorbed energy is then emitted at longer wavelengths through various types of mechanism.[1] Studies on potential luminescent metal complexes may contribute to our understanding of what is often termed 'the excited-state dimension' of coordination compounds and to the development of several novel branches of chemistry such as photochemistry, chemiluminescence and electron-transfer chemistry.[2] The practical applications of luminescent transition-metal complexes range from photochemical devices for interconversion of light and chemi-

cal energy[3] to environmental messengers[4,5] and luminescent sensors.[6–8]

Transition-metal complexes in excited states may also have a potential in synthesis, and coordinatively unsaturated complexes, particularly square-planar Pt[II] complexes, have been the subject of extensive studies; for surveys of recent references see Refs. 9–19. Excited states may be considered as electronic isomers of the ground state, and as such will exhibit particular chemical and physical properties.[20] Metal complexes being in the excited state may therefore react by alternative pathways and lead to products that may not be accessible by the complexes in their ground state.[21–23] Since an increase in the electron density on the metal atom appears to be a promising approach to accomplish the desired functions, various cyclometalated Pt[II] complexes have been used as model compounds. In this type of complex the platinum

---

† To whom correspondence should be addressed.

atom is linked to a carbanionic atom, a strong C-donor ligand. Complexes derived from 2-phenylpyridine and 2-(2'-thienyl)pyridine have therefore been studied extensively in recent years.[18]

With this kind of ligand the possibility for π-back-donation will be present. A tuning of the necessary energy gap between the emitting metal to ligand charge transfer, MLCT, and the non-emitting metal centered, MC, excited states is further possible by altering the ligands A and B, the charge of the complex, the counter-ion and also the solvent.[3]

Recently it has been shown that the precursor for most 2-(2'-thienyl)pyridine complexes, $Bu_4N^+[Pt(tpy)Cl_2]^-$, is more readily prepared than the corresponding compound from 2-phenylpyridine, $Bu_4N^+[Pt(ppy)Cl_2]^-$.[18] Since the availability of potentially luminescent species is important we have made a comparison of some complexes to examine whether the one substituted pyridine has an advantage to the other. In this work we have also included a comparison between complexes in which A and B represent the two two-coordinated ligands, 1,2-bis(diphenylphosphino)ethane, edp, and cis-1,2-bis(diphenylphosphino)ethene, etdp. According to Lever[24] the latter ligand has an electrochemical parameter, E_L, of 0.49 V which is quite high for phosphorus(III) ligands. It was of interest to examine whether it was possible to relate the redox properties of square-planar Pt^{II} complexes to the E_L parameters which had originally been derived from studies of octahedral complexes.[24]

Experimental

Materials. The preparation and characterization of $Bu_4N[Pt(ppy)Cl_2]$, **Ia**, $Bu_4N[Pt(tpy)Cl_2]$, **Ib**, [Pt(ppy)en]Cl, **IIa**, [Pt(tpy)en]Cl, **IIb**, [Pt(ppy)edt]ClO$_4$, **IIIa**, [Pt(tpy)edt]ClO$_4$, **IIIb**, $Bu_4N[Pt(ppy)(CN)_2]$, **IVa**, $Bu_4N[Pt(tpy)(CN)_2]$, **IVb** and [Pt(ppy)edp]Cl, **Va**, have been described[18] (en = 1,2-diaminoethane, edt =

1,2-bis(phenylthio)ethane, edp = 1,2-bis(diphenylphosphino)ethane).

[(1,2-Bis(diphenylphosphino)ethene)(2-phenylpyridinato-C^2,N')platinum(II)] chloride, [Pt(ppy)etdp]Cl, **VIa**, was made following the same procedure as for **Va**.[18] To a solution of $Bu_4N[Pt(ppy)Cl_2]$ in deoxygenated dichloromethane was added dropwise a solution of cis-1,2-bis(diphenylphosphino)ethene, Fluka, also dissolved in deoxygenated dichloromethane. After 1 h at room temperature the solvent was removed and the solid was washed with water. The final product was precipitated from a dichloromethane/benzene solution in 75% yield. M.p. 291 °C. ^{31}P NMR (CD$_3$OD), rel. to 85% H_3PO_4 in water: 46.0 ppm (J_{Pt-P} = 3754 Hz), 60.8 ppm (J_{Pt-P} = 1842 Hz). IR: ν_{Pt-P} = 505 and 553 cm^{-1}.

[(1,2-Bis(diphenylphosphino)ethene)(2-(2'-thienyl)pyridinato-C^3,N')platinum(II)] chloride, [Pt(tpy)etdp]Cl, **VIb**, was made in a similar way in 75% yield. M.p. 233 °C. ^{31}P NMR (CD$_3$OD): 44.3 ppm (J_{Pt-P} = 3742 Hz), 62.7 ppm (J_{Pt-P} = 2076 Hz). IR: ν_{Pt-P} = 505 and 553 cm^{-1}. The ^{1}H- and ^{13}C-NMR data, together with coupling constants of **VIa** and **VIb** in methanol-d_4, are summarized in Table 1. The coordination induced ^{13}C-shifts of the ppy and tpy parts of the studied compounds are listed in Table 2.

Instrumentation. UV/VIS spectra: Varian Cary 1 UV–visible spectrophotometer. ^{1}H-, ^{13}C- and ^{31}P-NMR: Bruker AM-400 WB spectrometer; δ in ppm relative to TMS for ^{1}H- and ^{13}C-NMR and relative to 85% H_3PO_4 for ^{31}P-NMR, J in Hz. IR: Perkin-Elmer 683 infrared spectrophotometer. The KBr technique was used throughout.

The instrumentation used to obtain emission spectra and luminescence lifetime data (estimated errors <10%) has been described.[19] A pulse nitrogen laser with λ_{exc} = 337 nm and a pulse halfwidth of 10 ns was used as an excitation source. The spectra were corrected for instrument response by the method of Parker and Rees.[25] Emission quantum yields were estimated by the optical

Table 1. ^{1}H, ^{13}C chemical shifts [δ(ppm) relative to TMS] and ^{195}Pt–^{13}C coupling constants (J/Hz) of the ppy and tpy parts of **VIa** and **VIb** in CD$_3$OD. For numbering of atoms see Scheme 1.

Compound		Atomic position										
		2	3	4	5	6	1'	2'	3'	4'	5'	6'
VIa	^{1}H		8.15	8.07	7.12	8.58 (28)			7.34 ^{a}	6.86	7.15	7.85
	^{13}C	169.2 (73)	121.9 (29)	143.1 ^{a}	125.7 (25)	154.2 (29)	148.9 (19)	160.8 ^{a}	140.4 (88)	132.2 (54)	127.7 ^{a}	126.0 (28)
							2'	3'	4'	5'		
VIb	^{1}H		7.66	7.96	7.00	8.35 (29)			6.53 (18)	7.31 (16)		
	^{13}C	163.6 (53)	120.3 (26)	143.8 ^{a}	124.0 (23)	153.7 (23)	149.6 ^{a}	164.8	136.7 (120)	130.9 ^{a}		

^{a} J_{Pt-C} not detectable due to lack of resolution or insufficient concentration.

Table 2. ^{13}C NMR coordination-induced shift, CIS,[a] and ^{195}Pt–^{13}C coupling constants (J/Hz).

Compound	a C(2')	b C(3')	a C(3')	b C(4')	a C(1')	b C(2')	a C(2)	b C(2)	a C(6)	b C(6)
I	17.6	17.8	4.3(54)	4.9(96)	1.6	−8.1	10.3(76)	10.6(77)	−0.2(27)	0.4(21)
II	18.6	20.1	4.2(61)	3.4(111)	4.0	−3.1	10.1	10.7	1.5(19)	1.8(16)
III	18.6	24.4	6.4(66)	3.7(105)	6.7(22)	3.3(12)	9.2	8.8	2.5(20)	2.9(17)
IV	31.1(804)	34.5	9.7(102)	8.0(126)	7.3(23)	0.7	10.7(72)	10.4	3.2(20)	3.4(31)
V	33.0(913)		10.5(87)		8.5(16)		10.4(66)		3.7(27)	
VI	32.7	34.3	10.6(88)	7.6(120)	8.5(19)	4.4	10.3(73)	9.8(53)	4.0(29)	3.6(23)

[a] $CIS = \delta_{complex} - \delta_{free\ ligand}$ in the same solvent.

dilution method[26] using $[\text{Rubipy}_3]^{2+}$ [27] ($\Phi_{em} = 0.028$) and fluorescein[28] ($\Phi_{em} = 0.85$) as standards and were corrected for the difference in refractive index of the solvents. The total error was estimated to be less than 30%. Electrochemical measurements were carried out in solutions in dimethylformamide, DMF, under argon with Bu_4NClO_4 as supporting electrolyte using standard SVA-1B and N307/1-XY recorders. Cyclic voltammograms were obtained using a Pt wire, glassy carbon and Hg (Au-amalgam) as working electrodes; a Pt counterelectrode and a Ag/Ag^+ electrode functioned as reference electrodes. The scanning rate was $100\ mV\ s^{-1}$. The ferrocenium (Fc^+)/ferrocene (Fc) couple was used as a reference redox system under the same experimental conditions. The E° of the Fc^+/Fc couple was assumed to be as measured in water; i.e. 0.400 V vs. NHE.[29]

Results and discussion

The compounds considered in the present study were readily isolated in good yields, more than 60%, from the Bu_4N^+ salts of $[\text{Pt(ppy)Cl}_2]^-$ and $[\text{Pt(tpy)Cl}_2]^-$, generally abbreviated $Bu_4N[Pt<N-C>Cl_2]$.[18] Pure samples of $[\text{Pt(tpy)edp}]^+$ salts could not be obtained as viewed by the ^{31}P-NMR spectra. All compounds are stable in the solid state and when dissolved in dichloromethane, chloroform, acetone, dimethylformamide and water. The salts of $[Pt<N-C>Cl_2]^-$ and $[Pt<N-C>(CN)_2]^-$ were found to decompose slowly in acetonitrile, preventing voltammetric studies from being performed in this solvent.

The two new complexes derived from etdp, VIa and VIb, were characterized by IR, UV–visible and various types of NMR techniques as previously described;[18] cf. Tables 1 and 2. As viewed by the ^{31}P-NMR shifts the two phosphorus atoms are significantly different, 46.0 and 60.8 ppm in the ppy complex and 44.3 and 62.7 ppm in the tpy complex, as compared with − 23.1 ppm for pure etdp.[30] The average shift difference from the pure diphosphine, ca. 76 ppm, is significantly larger than the corresponding difference for $[\text{Pt(ppy)edp}]ClO_4$, ca. 64 ppm.[18,30] This may suggest that etdp acts as a better donor than edp toward the platinum atom. The ^{195}Pt–^{31}P spin coupling constants, J_{Pt-P}, however, are fairly similar. According to Crociani et al.[31] the upfield phosphorus

atom with the largest coupling constant is trans to the nitrogen atom in the cyclometalated ligands. It was not possible to determine the C = C frequency in the etdp complexes owing to the presence of several strong bands in the $1600\ cm^{-1}$ region.

The ^{1}H-NMR data, Table 1 and Ref. 18, indicate that the proton shifts in $[Pt<N-C>AB]$ are quite sensitive to the nature of the A and B ligands. However, the large number of contributing factors to these parameters does not permit definite conclusions to be made with regard to the donor and acceptor properties of the ligands. In this respect the ^{13}C-shift data, particularly the coordination induced ^{13}C-shifts, CIS, Table 2, are more informative. $J_{Pt-C4'}$-values in the tpy compounds are generally larger than the corresponding $J_{Pt-C3'}$-values in the ppy series; the ratio J_{tpy}/J_{ppy} being ca. 1.7. Based upon the difference in $J_{Pt-C4'}$ and $J_{Pt-C3'}$ one may conclude that the platinum atom is more strongly linked to the thienyl part of the tpy ligand than to the phenyl part of ppy. However, since the Pt-C2'–C3' and Pt-C3'–C4' bond angles in the two types of complex are significantly different, ca. 128 and 135°, respectively,[32,33] the larger coupling constant in the tpy complexes may entirely be explained by the dihedral angular dependence of J_{tpy}/J_{ppy}. The ratio can be compared with the data for the excitation energy of the lower MLCT excited state, $\Delta E_{tpy}/\Delta E_{ppy} \approx 0.8$, as deduced from the spectroscopic measurements (Tables 3 and 4). Apparently, the larger value of $J_{Pt-C4'}$ is paralleled by a smaller excitation energy.

The deshielding of C2', C3' and C6 (ppy) and of C3', C4' and C6 (tpy) suggests a 'spectrochemical order' of the A and B ligands equal to etdp $\approx$ edp > $(CN^-)_2$ > edt $\approx$ en > $(Cl^-)_2$, an order consistent with the known donor and acceptor properties of the ligands. A higher π-acceptor ability will remove electron density from the $<N-C>$ ligand and lead to a larger degree of deshielding. A comparison of the CIS values for C1'(ppy) and C2'(tpy) may not be valid, since the configuration of the tpy ligand is changed from cis to trans upon complexation.[18]

Electrochemistry. The nature of the highest occupied molecular orbital (HOMO) and lowest unoccupied molecular orbital (LUMO) of the complex ions was examined using cyclic voltammetry in DMF. From the cyclic voltammograms the $E_{1/2}$-values were determined for revers-

Table 3. Reduction and oxidation potentials in DMF vs. Fc^+/Fc (0.1 M in TBAP).

Compound	Reduction $-E_{1/2}$ $(\Delta E_p)^a$		Oxidation $E_p^{\ b}$		
	ppy	tpy	ppy	tpy	$E_L^{\ c}$
I	2.47(0.07)	2.49(0.07)	0.36	0.39	−0.24
II	2.22(0.08)	2.25(0.08)	0.84	0.86	0.06
III	1.77(0.10)	1.82(0.10)	1.21	1.11	0.36
IV	2.36(0.07)	2.36(0.07)	0.65	0.66	0.02
V	1.83(0.07)		0.70		0.36
VI	1.79(0.08)	1.76(0.08)	0.70	0.48	0.49

^{a} ΔE_p is defined as the difference between the anodic and cathodic waves of the electrochemical process in absolute value.
^{b} Irreversible wave. ^{c} Ligand electrochemical parameters from Ref. 24.

ible and quasi-reversible reduction, while the E_p-values were determined for irreversible oxidation; cf. Table 3. Since Pt^I and Pt^{III} complexes are unstable species,[34] metal-centered oxidation and reduction processes of Pt^{II} compounds are in principle expected to exhibit an irreversible behaviour. For complexes with cyclometalated <N–C> ligands like ppy and tpy, however, reduction is expected to be reversible or quasi-reversible, since delocalized π^*-orbitals are involved.[11] Oxidation processes may additionally involve the heteroatom in the ligands and are expected to be irreversible. The results obtained for the cyclometalated Pt^{II} complexes (Table 3) are in agreement with the localized molecular-orbital approach. All complexes show a ligand-centered reduction wave, $E_{1/2}$, ranging from −1.8 to −2.5 V, which can be assigned to electron transfer to the π^*-orbital localized on the cyclometalated ligand. The shift of the reduction wave towards more negative potentials when changing the ligands in the series etdp, edp, edt, en and Cl^- is therefore in agreement with the NMR data with regard to the shielding of the C(6) carbon atom of the pyridine ring (Fig. 1). The deviation in this plot for the two dicyano
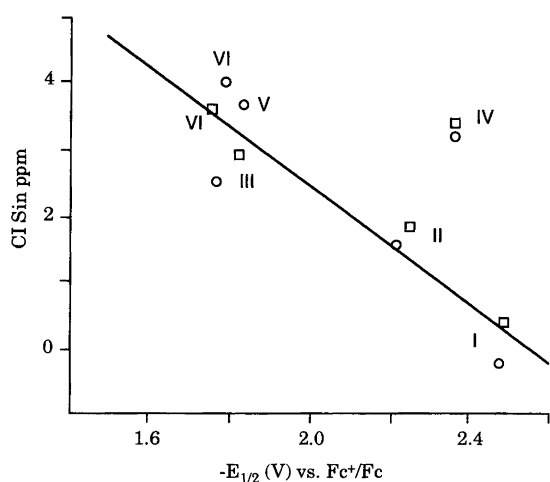
complexes, IVa and IVb, can probably be attributed to additional deshielding of the C(6) carbon atom due to anisotropic effects by the cyano ligands.

The electron-withdrawing ability of the 'PtAB' moiety can also be considered in terms of the so-called 'ligand electrochemical parameter', E_L.[24] This parameter is defined as one-sixth of the Ru^{III}/Ru^{II} potential for RuL_6 species in acetonitrile. Based on the E_L parameter it is possible to predict the M^{x}/M^{x-1} redox potentials when the contributions of all ligands are assumed to be additive. According to this approach a correlation between ligand-centered reduction potentials of [Pt<N–C>AB] and the sum of the E_L parameters of the A and B ligands is to be expected;[35] cf. Fig. 2, lower plot. It is notable that the two dicyano complexes do not deviate in this plot. The observed oxidation waves are completely irreversible and can in most cases be assigned to a metal-centered $Pt^{II} \rightarrow Pt^{III}$ oxidation followed by a fast chemical reaction.[36] This assignment is strengthened by the observed
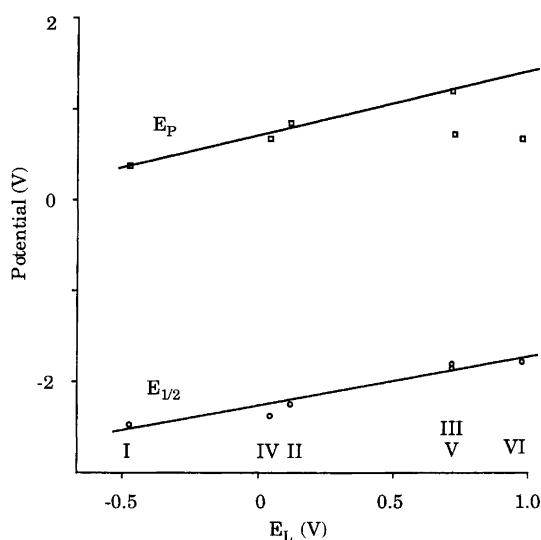

Fig. 1. Plot of CIS values, $\Delta = \delta_{complex} - \delta_{free\ ligand}$, for the C(6) atom of the cyclometalated ligands versus the values of the reduction potentials of [Pt<N–C>AB]. (Circles for ppy complexes, squares for tpy complexes).

Fig. 2. Plot of experimental oxidation and reduction potentials of [Pt<N–C>AB] (average values for ppy and tpy complexes) versus the sum of the electrochemical parameters, E_L, of the A and B ligands.

Table 4. Absorption spectra of [Pt<N-C>AB]. λ_{max}/nm, $\varepsilon \times 10^{-3}$.

AB	Solvent	3MLCT $(d_{Pt}-\pi^*_{<N-C>})$		1MLCT $(d_{Pt}-\pi^*_{<N-C>})$		1LC $(\pi_{<N-C>}-\pi^*_{<N-C>})$	
		ppy	tpy	ppy	tpy	ppy	tpy
Cl⁻,Cl⁻	DMF	490(0.058)	565(0.033) 546(0.030) 521(0.050)	380ᵃ(4.0) 371(4.3)	455ᵃ(1.7) 428(2.2)	330ᵃ(4.5)	340(9.0) 298(17.0)
	MeOH	450ᵃ(0.13)	556(0.027) 536(0.027) 513(0.040)	400ᵃ(0.8) 365(4.0)	420(2.4) 403(2.6) 360(4.3)	326ᵃ(5.0) 314ᵃ(5.0)	328ᵃ(8.5) 300ᵃ(12.5) 286(13.4)
en	DMF	477(0.022) 445(0.041)	553(0.006) 535ᵃ(0.007) 518ᵃ(0.010) 509ᵃ(0.011)	395ᵃ(1.3) 375(1.8)	421ᵃ(1.9) 401(2.4)	325(4.5)	325ᵃ(5.85) 310ᵃ(7.25) 295(8.2)
	MeOH	474(0.015) 441(0.041)	553ᵃ(0.011) 534(0.012) 514ᵃ(0.017) 492ᵃ(0.020)	368(1.7)	419ᵃ(3.0) 401(3.7)	320(5.1) 308ᵃ(5.6)	323ᵃ(9.3) 308ᵃ(11.6) 294(13.9)
edt	DMF	470(0.008) 440ᵃ(0.027)	530ᵃ(0.021)	357(2.5)	391(2.6) 374(2.8)	325(6.5) 317(6.5)	318ᵃ(8.7) 298(10.1)
	MeOH	470(0.004) 438(0.011)		354(2.5)	412ᵃ(3.4) 394(4.9)	323(6.7) 314(6.8)	319ᵃ(11.5) 312(11.6)
CN⁻,CN⁻	DMF	475(0.017) 443(0.032)	550(0.016) 532ᵃ(0.018) 518ᵃ(0.026) 507ᵃ(0.030)	380ᵃ(1.7) 340(4.0)	398(3.1)	325(5.6)	330(9.2) 308ᵃ(11.7) 299(12.5)
	MeOH	470(0.004) 438(0.019)	546(0.024) 528ᵃ(0.008) 505ᵃ(0.039)	363(2.5)	408ᵃ(3.3) 393(3.8)	325(7.6)	323(9.6) 301ᵃ(11.3) 291(13.1)
edp	DMF	470(0.007) 435ᵃ(0.023) 425(0.036)		361(3.5)		382(7.8) 322(7.6)	
	MeOH	470(0.008) 435ᵃ(0.012) 425(0.014)		361(2.6)		330(6.3) 321(6.2)	
etdp	DMF	470(0.008) 439(0.013)	552(0.009) 506ᵃ(0.016)	372ᵃ(1.9) 359(2.6)	395(2.7)	330(6.1) 319(6.1)	325ᵃ(4.9) 313ᵃ(6.9) 299(8.1)
	MeOH			375ᵃ(1.4) 364ᵃ(2.0) 356(2.3)	395(3.4)	330(5.4) 319(5.3)	329ᵃ(5.7) 311ᵃ(9.4) 298(10.4)

ᵃ Shoulder.

correlation between E_P and the sum of the E_L parameters[24] (Fig. 2, upper plot), which is expected for redox processes occurring within the nonbonding or weakly π-bonding (or antibonding) metal-centered HOMOs. However, both [Pt<N–C>edp]⁺ and [Pt<N–C>etdp]⁺ show an oxidation wave at E_P from 0.5 to 0.7 V, far below the expected values; cf. Fig. 2. Moreover, these values are close to the irreversible oxidation waves observed for free edp and etdp ligands (Fig. 3). Apparently, the oxidation wave for [Pt<N–C>edp]⁺ and [Pt<N–C>etdp]⁺ can be assigned to edp and etdp ligand-centered oxidation processes, probably due to steric hindrance for interaction between the metal orbitals and the electrode.

Owing to the irreversibility of the oxidation processes,

the experimental oxidation potentials cannot give reliable information about the energy position of the HOMO in the complexes. The electrochemical data in Table 3 and Fig. 2, however, show that the reduction and oxidation potentials of [Pt(ppy)AB] and [Pt(tpy)AB] are quite similar. This observation suggests that the energy of the HOMO and the LUMO remains relatively fixed in the two types of complexes. The linearity in the plots in Fig. 2 suggests that redox properties of square-planar complexes can be predicted with considerably reliability from Lever's E_L-values. The rather similar slopes in the two plots, ca. 0.65 for oxidation and ca. 0.55 for reduction, suggest that the energy gap between the HOMO and the LUMO of the complexes is only slightly dependent upon the nature of the A and B ligands.
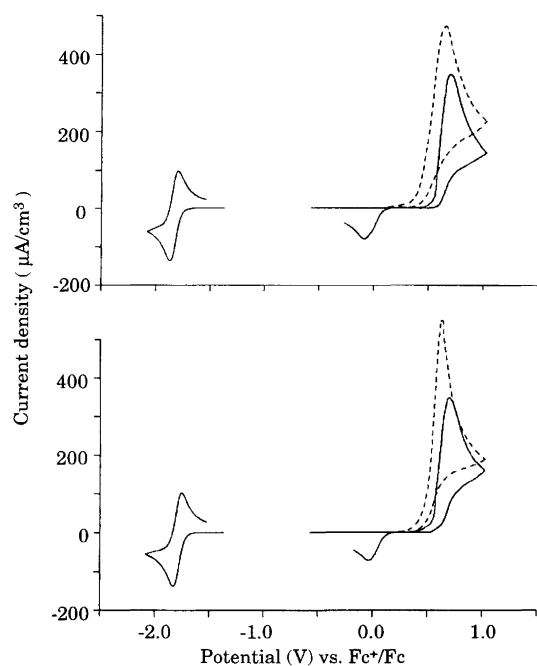
Fig. 3. Cyclic voltammograms of [Pt(ppy)edp]⁺ (——) and edp (— — —), upper curves, and of [Pt(ppy)etdp]⁺ (——) and etdp (— — —), lower curves, in DMF at room temperature.

Electronic spectroscopy. The absorption and emission spectra of [Pt(ppy)Cl$_2$]⁻ and [Pt(ppy)en]⁺ have been reported.[19] Table 4 contains a list of absorption features

for the two series of complexes. The emission data are summarized in Table 5.

The absorption and emission spectra for each member in the two series are in principle quite similar to the spectra obtained for the bis-cyclometalated complexes, [Pt<N–C>$_2$], and the same electronic assignments are suggested.[12,37] Based on the localized molecular orbital approach, the intense absorption bands observed in the visible and near-UV spectral region (Table 4) are assigned to two types of spin-allowed electronic transitions; ligand centered, ¹LC, ($\pi_{<N-C>}$–$\pi^*_{<N-C>}$) and ¹MLCT (d$_{Pt}$–$\pi^*_{<N-C>}$). A much weaker, highly structured absorption in the visible region (Fig. 4) is attributed to the corresponding singlet–triplet ³MLCT transition. The vibrational satellite structure observed in the absorption spectra of [Pt(tpy)AB] and [Pt(ppy)AB] at 1500 ± 80, 1180 ± 70 and 690 ± 80 cm⁻¹ and the single vibrational satellite at 1540 ± 30 cm⁻¹ can be attributed to high-energy vibrations of the cyclometalated ligands. The splitting for spin-allowed and spin-forbidden MLCT transitions calculated from the highly structured absorption spectra of the [Pt(tpy)AB] complexes, 5600 ± 700 cm⁻¹, is in agreement with the expected splitting, ca. 5000 cm⁻¹, for MLCT transitions of cyclometalated Pt^{II} complexes.[38]

The assignment of the low-energy absorption bands to a ³MLCT transition is confirmed by the long-lived electronic emission, and the electronic origin seems to overlap well with the absorption origin, cf. Fig. 4. The vibrational satellite structure, 660 ± 20, 1040 ± 50 and

Table 5. Properties of the lowest excited state of the Pt^{II} complexes.

Comp.	Solv.	293 K							77 K				
		λ^a /nm	τ^b /µs	$\Phi^b \times 10$	τ_r /µs	$k^c \times 10^{-4}$ /s⁻¹	$E^{red}_{1/2}$ /V	$-E^{ox}_{1/2}$ /V	λ^a /nm	τ /µs	$\Phi \times 10$	τ_r /µs	$k^c \times 10^{-4}$ /s⁻¹
Ia	MeOH	e							480	13	9.0	10	1
	DMF	e					0.1	2.2	491	7.9	6.5	10	5
IIa	MeOH	485	10	3.5	30	6			480	18	4.9	40	2
	DMF	487	1.7	0.6	30	60	0.4	1.7	481	15	7.2	20	2
IIIa	MeOH	481	1.6	d					475	40	4.8	80	1
	DMF	493	3.3	d			0.8	1.3	476	29	7.1	40	1
IVa	MeOH	480	2.5	d					475	26	4.0	60	2
	DMF	484	1.3	d			0.3	1.9	475	22	7.5	30	1
Va	MeOH	e							475	61	3.1	200	1
	DMF	e					0.8	1.9	477	50	6.5	80	1
VIa	MeOH	e							476	66	7.0	90	0.5
	DMF	e					0.8	1.9	478	56	9.5	60	0.1
Ib	MeOH	556	9.0	1.4	60	10			557	17	2.2	80	5
	DMF	565	9.1	1.5	60	9	−0.3	1.8	560	16	3.7	40	4
IIb	MeOH	555	18	2.5	70	5			556	16	2.1	80	4
	DMF	561	10	3.5	30	10	0.0	1.4	556	8.8	1.0	90	3
IIIb	MeOH	559	13	1.2	110	7			553	36	1.5	240	2
	DMF	566	12	2.0	56	9	0.4	1.1	559	29	3.5	80	2
IVb	MeOH	556	34	2.2	140	3			554	29	2.8	100	2
	DMF	558	35	3.3	100	4	−0.1	1.4	553	19	3.1	60	2
VIb	MeOH	560	27	d					554	58	2.8	200	1
	DMF	565	24	d			0.5	1.7	556	48	3.1	150	1

^{a} Highest-energy feature of the luminescence emission maxima. ^{b} Deareated solution. ^{c} Non-radiative rate constant. ^{d} Photochemically unstable. ^{e} Emission too weak.
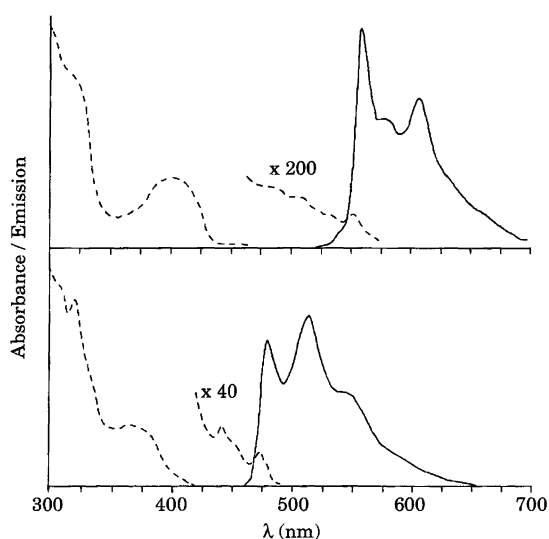
Fig. 4. Absorption and emission spectra of [Pt(tpy)en]$^+$, upper curves, and [Pt(ppy)en]$^+$, lower curves, in DMF at room temperature.

1400 ± 20 cm^{-1}, tpy modes, and 390 ± 30, 710 ± 20, 1130 ± 20 and 1450 ± 20 cm^{-1}, ppy modes, is in agreement with recently reported high-resolution spectroscopic data for cyclometalated Rh^{III}, Ir^{III} and Pd^{II} complexes with ppy and tpy ligands.[38-41] The radiative lifetimes, τ_r, range from 10 to 240 μs and are calculated from the measured emission lifetime, τ, and the quantum yield, Φ (Table 5). These values are consistent with dipole-allowed spin-forbidden transitions. The emission spectra show a solvatochromic effect as observed for the corresponding MLCT absorption bands.

It should be noted that for cyclometalated Pt^{II} complexes, as for Ir^{III}, Rh^{III} and Pd^{II} complexes with a high degree of covalency in the metal–ligand bonds, the classification of the excited states based on the localized molecular-orbital approach can only be used as a first approximation. In the case of homoleptic cyclometalated Pt^{II} and Pd^{II} complexes,[37,42,43] the LUMOs are the stabilized ligand hybrid MOs, $\pi^*_{<N-C>}$, whereas the HOMOs are a mixture between destabilized metal d$_{xy}$ and ligand $\pi_{<N-C>}$ states. Thus, the character of the lowest excited states, predominantly LC for Pd^{II} complexes and with an admixture of MLCT for Pt^{II} complexes, differs only in the extent of mixing of d$_{xy}$ and $\pi_{<N-C>}$ orbitals.[41] The limitations in the usual classification scheme for the assignment of the lowest excited states, MLCT or LC,
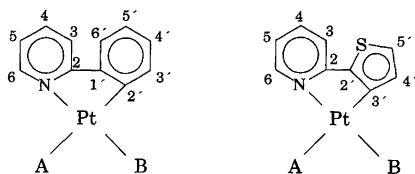
Scheme 1.

have also been discussed for [Ir(ppy)$_2$bpy]$^+$ and [Ir(tpy)$_2$bpy]$^+$.[44]

The electronic spectroscopy data for the studied Pt^{II} complexes suggest that the character of the lowest excited state of the [Pt<N–C>AB] complexes is due to both the cyclometalated <N–C> ligand and the A and B ligands. In agreement with the NMR data, the increase in π-back-bonding from the electron rich metal to the A and B ligands, etdp $\approx$ edp > (CN$^-$)$_2$ > edt $\approx$ en > (Cl$^-$)$_2$, leads to a number of remarkable features in the absorption and emission data: (i) there is a blue shift of the spin-forbidden MLCT absorption and emission bands; (ii) the solvatochromic effect is decreased; (iii) the radiative lifetimes are increased and the extinction coefficients are decreased. These trends can be attributed to an increasing admixture of the cyclometalated ligand states, $\pi_{<N-C>}$, to the HOMOs leading to a corresponding increase in the contribution of the LC-character of the lowest excited state of the complexes.

When replacing ppy with tpy a red shift of the MLCT structured absorption and emission bands by about 3000 cm^{-1} is observed. However, the redox potentials for the two series of the cyclometalated complexes are most similar; cf. Table 3. The highest-energy emission and the lowest-energy absorption maxima are most similar for the two series and depend only slightly on the donor and acceptor properties of the A and B ligands and the polarity of the solvent. The extinction coefficients of [Pt(tpy)AB] are smaller and the radiative lifetimes are longer as compared to the values for [Pt(ppy)AB]; on average $\varepsilon_{(ppy)}/\varepsilon_{(tpy)} = 1.7 \pm 1$ and $\tau_{r(tpy)}/\tau_{r(ppy)} = 2.6 \pm 1$. Apparently, the lowest excited state of the tpy complexes has more contribution of the π-character of the cyclometalated ligand as compared with the corresponding ppy complexes.

The quenching of the luminescence of [Pt(ppy)Cl$_2$]$^-$ and [Pt(ppy)en]$^+$ by an increase in temperature has been assigned to the thermally activated population of the upper-lying MC excited states followed by fast radiationless processes.[19] This leads to a dependence of the parameters of the luminescence of the [Pt(ppy)AB] complexes in fluid solutions at room temperature on the ligand field strength of the A and B ligands (Table 5). Contrary to most [Pt(ppy)AB] complexes, the [Pt(tpy)AB] complexes show strong emission both at 77 K and at room temperature. This indicates that when replacing ppy with tpy, the energy of the lowest emitting excited state (ca. 3000 cm^{-1}) is lowered and will cause an increase in the energy gap between the emitting and the upper lying MC excited state.

Based upon the spectroscopic and electrochemical data the redox potentials of the excited state of cyclometalated Pt^{II} complexes can be estimated; cf. Table 5. The data show that the lowest long-lived excited state of the cyclometalated Pt^{II} complexes are both good reductants and oxidants. Given the high luminescence quantum yields and long lifetimes of [Pt(ppy)en]$^+$ and the [Pt(tpy)AB] complexes in fluid solution at room tempera-

ture, it is not difficult to envisage that these complexes will possess rich photochemistry.

Conclusion

A comparison of cyclometalated Pt^{II} complexes derived from 2-phenylpyridine and 2-(2'-thienyl)pyridine has revealed that the lowest excited state in the latter complexes has a larger contribution of the π-character of the cyclometalated ligand. A similar effect can be obtained by increasing the π-acceptor properties of the A and B ligands. While the reduction and oxidation potential of the ground state and the lowest excited state remain essentially unaltered, the tpy complexes show significantly higher luminescent character at room temperature. Although the quantum yield of the studied ppy complexes is slightly higher at 77 K than for the corresponding tpy complexes, futural studies may preferably be performed with 2-(2'-thienyl)pyridine as the cyclometalated ligand.

The E_L parameters seem to be valuable when attempting to predict the redox properties of square planar platinum complexes. However, when oxidation potentials are to be considered, deviations can be expected when the ligands contain readily oxidizable heteroatoms.

References

1. Ferraudi, G. J. *Elements of Inorganic Photochemistry*, Wiley, New York 1988.
2. Fox, M. A. and Chanon, M., Eds., *Photoinduced Electron Transfer*, Elsevier, Amsterdam 1989.
3. Balzani, V. and Scandola, V. *Supramolecular Photochemistry*, Ellis Horwood, Chichester 1991.
4. Lees, A. J. *Chem. Rev. 87* (1987) 711.
5. Kalyanasundaram, K. *Photochemistry in Microheterogeneous Systems*, Academic Press, New York 1987.
6. Wolfbeis, O. S., Posch, H. E. and Kroneis, H. W. *Anal. Chem. 57* (1985) 2556.
7. Wolfbeis, O. S., Weis, L. J., Leiner, M. J. P. and Ziegler, W. E. *Anal. Chem. 60* (1988) 2028.
8. Bacon, J. R. and Demas, J. N. *Anal. Chem. 59* (1987) 2780.
9. Bevilacqua, J. M., Zuleta, J. A. and Eisenberg, R. *Inorg. Chem. 33* (1994) 258.
10. Ballardini, R., Gandolfi, M. T., Prodi, L., Ciano, M., Balzani, V., Kohnke, F. H., Shahriari-Zavareh, H., Spencer, N. and Stoddart, J. F. *J. Am. Chem. Soc. 111* (1989) 7072.
11. Maestri, M., Deuschel-Cornioley, C. and von Zelewsky, A. *Coord. Chem. Rev. 111* (1991) 117.
12. Sandrini, D., Maestri, M., Ciano, M. and Balzani, V. *Gazz. Chim. Ital. 118* (1988) 661 and Maestri, M., Sandrini, D.,

13. Balzani, V., Chassot, L., Jolliet, P. and von Zelewsky, A. *Chem. Phys. Lett. 122* (1985) 375.
13. Scolaro, L. M., Alibrandi, G., Romeo, R., Ricevuto, V. and Campagna, S. *Inorg. Chem. 31* (1992) 2074.
14. Craig, C. A., Garces, F. O., Watts, R. J., Palmans, R. and Frank, A. J. *Coord. Chem. Rev. 97* (1990) 193.
15. Blanton, C. B., Murtaza, Z., Shaver, R. J. and Rillema, D. P. *Inorg. Chem. 31* (1992) 3230.
16. Chan, C.-W., Lai, T.-F., Che, C.-M. and Peng, S.-M. *J. Am. Chem. Soc. 115* (1993) 11245.
17. Ivanova, M. E. and Shagisultanova G. A. *Russ. J. Inorg. Chem. 36* (1991) 815.
18. Kvam, P.-I. and Songstad, J. *Acta Chem. Scand. 49* (1995) 313.
19. Kvam, P.-I., Puzyk, M. V., Balashev, K. P. and Songstad, J. *Acta Chem. Scand. 49* (1995) 335.
20. Adamson, A. W. *J. Chem. Ed. 60* (1983) 797.
21. Gerasimov, O. V. and Parmon, V. N. *Russ. Chem. Rev. 61* (1992) 154.
22. Sandrini, D., Maestri, M., Balzani, V., Chassot, L. and von Zelewsky, A. *J. Am. Chem. Soc. 109* (1987) 7720.
23. von Zelewsky, A., Suckling, A. P. and Stoeckli-Evans, H. *Inorg. Chem. 32* (1993) 4585.
24. Lever, A. B. P. *Inorg. Chem. 29* (1990) 1271.
25. Parker, C. A. and Rees, W. T. *Analyst (London) 85* (1960) 587.
26. Demas, J. N. and Crosby, G. A. *J. Phys. Chem. 75* (1971) 991.
27. Nakamuru, K. *Bull. Chem. Soc. Jpn. 55* (1982) 2697.
28. Demas, J. N. and Crosby, G. A. *J. Am. Chem. Soc. 92* (1970) 7262.
29. Gagné, R. R., Koval, C. A. and Lisensky, G. C. *Inorg. Chem. 19* (1980) 2854.
30. Colquhoun, I. J. and McFarlane, W. *J. Chem. Soc., Dalton Trans.* (1982) 1915.
31. Crociani, B., Bianca, F. D. and Giovenco, A. *J. Organomet. Chem. 361* (1989) 255.
32. Giordano, T. J. and Rasmussen, P. G. *Inorg. Chem. 14* (1975) 1628.
33. Kvam, P.-I., Engebretsen, T., Maartmann-Moe, K. and Songstad, J. *Acta Chem. Scand. Submitted.*
34. Cotton, F. H. and Wilkinson, G. *Advanced Inorganic Chemistry*, Wiley, New York 1988, pp. 917–937.
35. Dodsworth, E. S., Vlcek, A. A. and Lever, A. B. P. *Inorg. Chem. 33* (1994) 1045.
36. Bonafede, S., Ciano, M., Bolleta, F., Balzani, V., Chassot, L. and von Zelewsky, A. *J. Phys. Chem. 90* (1986) 3836.
37. Schwarz, R., Gliemann, G., Chassot, L., Joliet, P. and von Zelewsky A. *Helv. Chim. Acta 72* (1989) 224.
38. Maestri, M., Sandrini, D., Balzani, V., von Zelewsky, A. and Joliet, P. *Helv. Chim. Acta 71* (1988) 134.
39. Zilian, A. and Güdel, H. U. *Inorg. Chem. 31* (1992) 830.
40. Colombo, M. G. and Güdel, H. U. *Inorg. Chem. 32* (1993) 3081.
41. Yersin, H., Schutzenmeier, S., Wiedenhofer, H. and von Zelewsky, A. *J. Phys. Chem. 97* (1993) 13496.
42. Schwarz, R., Gliemann, G., Joliet, P. and von Zelewsky, A. *Inorg. Chem. 28* (1989) 742.
43. Schwarz, R., Gliemann, G., Joliet, P. and von Zelewsky, A. *Inorg. Chem. 28* (1989) 1053.
44. Colombo, M. G., Hauser, A. and Güdel, H. U. *Inorg. Chem. 32* (1993) 3088.